2015 International Symposium on Nonlinear Theory and its Applications
NOLTA2015, Kowloon, Hong Kong, China, December 1-4, 2015

Restricted normal mode analysis of the P-mode Intrinsic Localized Mode

Edmon Perkins and Balakumar Balachandran

Department of Mechanical Engineering, University of Maryland
Glenn L. Martin Hall, College Park, MD 20712, USA
Email: edmon@umd.edu

Abstract—Nonlinearity and discreteness can cause energy localizations called intrinsic localized modes (ILMs) in a coupled oscillator array. A spatial physical manifestation of this localization is the P-mode ILM, which is an anti-symmetric spatial mode. By contrast, the ST-mode is a symmetric spatial mode. In this effort, the P-mode is studied by means of the restricted normal mode approach, and insights gained into the dynamics of this localization are discussed.

1. Introduction

Intrinsic localized modes are nonlinear phenomena associated with coupled oscillator arrays. They are large amplitude oscillations, which may cause damage to an array. However, if properly understood, these energy localizations may be used advantageously in applications, for example, for sending packets of energy through a certain oscillator channel in an array. Given that bistable dynamic states of a Duffing oscillator have been utilized in the implementation of binary memory operations [1], this work may have relevance for memory operation procedures as well. Additionally, the localization phenomenon in a coupled oscillator system can serve as a paradigm for localization in other systems.

Experimentally, ILMs have been found to occur in a range of physical systems, including macro-scale cantilever arrays [2], micro-scale cantilever arrays [3, 4], photonic lattices [5], and Josephson junctions [6]. Analytical and numerical investigations into this phenomenon have also been carried out. The restricted normal mode approach has been used to investigate the ST-mode, and it has been discussed that the ST-mode may be considered as a nonlinear vibration mode of an array [7]. The effect of cubic coupling on the ST-mode was further explored in recent work [8], wherein the influence of noise on this spatial shape has also been examined. The effects of noise on an ST-mode ILM has been explored both experimentally and numerically in a recent work [9]. In another related work, it has been discussed that the stability changes of ST- and P-mode ILMs are governed by the intersite nonlinearity and onsite nonlinearity [10].

In this paper, a restricted normal mode approach is used to study the P-mode ILM. This approach is similar to that employed in previous efforts [7, 8], wherein the focus was on the ST-mode. Numerical studies are used to glean information about the dynamics of the P-mode ILM. The rest of this paper is structured as follows. In Section 2, the restricted normal mode approach is detailed. The P-mode profile is predicted by using this method. In Section 3, the system of equations for the coupled oscillator array are numerically solved, by using the predicted P-mode profile as the initial condition. Concluding remarks are presented in the last section.

2. Restricted Normal Mode

The equations of motion for the i^{th} oscillator in the coupled oscillator array is given by

$$\begin{aligned}\ddot{x}_i + c_i\dot{x}_i + \alpha_1 x_i + \beta_1 x_i^3 + \alpha_2(x_i - x_{i+1}) + \alpha_2(x_i - x_{i-1}) \\ +\beta_2(x_i - x_{i+1})^3 + \beta_2(x_i - x_{i-1})^3 = Fcos(\Omega t)\end{aligned} \tag{1}$$

Here, α_1 is the onsite linear stiffness term, α_2 is the intersite linear coupling term, β_1 is the onsite cubic stiffness term, β_2 is the intersite cubic coupling term, c_i is the damping coefficient that is positive valued, F is the forcing amplitude, and Ω is the forcing frequency. Note that the mass coefficient has been normalized.

The construction of the restricted normal mode for the P-mode requires a different set of initial assumptions than those needed for the ST-mode, since the P-mode is anti-symmetric while the ST-mode is symmetric. In the group's prior work, the restricted normal mode approach was used for study of the ST-mode. In this symmetric mode, the peak of the ILM is located at x_0, and it is assumed that $x_{+1} = x_{-1}$ and that the ± 2 oscillators have negligible influence on the ST-mode ILM profile. By contrast, for the P-mode, the center of the ILM is between oscillators ± 1. The following assumptions are made to proceed with this method: 1) $x_{-1} = -x_{+1}$, 2) $x_{-2} = -x_{+2}$, and 3) $x_{-3} = 0 = x_{+3}$. The first two assumptions ensure that the mode shape is anti-symmetric, while the last assumption means that the ± 3 oscillators have neglible influence on the P-mode ILM profile. It should also be noted that there is no central (i.e., 0^{th}) oscillator with a peak response in this construction; there is a zero crossing between the ± 1 oscillators. After setting the forcing to zero and considering the undamped case, the equations of motion for oscillators 1 and 2 (which are involved in the P-mode ILM) may be written as follows:

$$\begin{cases} \ddot{x}_1 + \alpha_1 x_1 + \beta_1 x_1^3 + \alpha_2(x_1 - x_2) + \alpha_2(x_1 - x_{-1}) \\ \quad +\beta_2(x_1 - x_2)^3 + \beta_2(x_1 - x_{-1})^3 = 0 \\ \ddot{x}_2 + \alpha_1 x_2 + \beta_1 x_2^3 + \alpha_2(x_2 - x_3) + \alpha_2(x_2 - x_1) \\ \quad +\beta_2(x_2 - x_3)^3 + \beta_2(x_2 - x_1)^3 = 0 \end{cases} \tag{2}$$

By applying assumptions (1)−(3) to Eqs.(2), the following set of equations is produced:

$$\begin{cases} \ddot{x}_1 + \alpha_1 x_1 + \beta_1 x_1^3 + \alpha_2(x_1 - x_2) + \alpha_2(x_1 + x_1) \\ \quad +\beta_2(x_1 - x_2)^3 + \beta_2(x_1 + x_1)^3 = 0 \\ \ddot{x}_2 + \alpha_1 x_2 + \beta_1 x_2^3 + \alpha_2(x_2 - 0) + \alpha_2(x_2 - x_1) \\ \quad +\beta_2(x_2 - 0)^3 + \beta_2(x_2 - x_1)^3 = 0 \end{cases} \tag{3}$$

After rearranging Eqs. (3), the following set of differential equations, which govern the shape of the P-mode ILM, are found.

$$\begin{cases} \ddot{x}_1 + \alpha_1 x_1 + (\beta_1 + 8\beta_2)x_1^3 + \alpha_2(3x_1 - x_2) \\ \quad +\beta_2(x_1 - x_2)^3 = 0 \\ \ddot{x}_2 + \alpha_1 x_2 + (\beta_1 + \beta_2)x_2^3 + \alpha_2(2x_2 - x_1) \\ \quad +\beta_2(x_2 - x_1)^3 = 0 \end{cases} \tag{4}$$

Following along the lines of the group's earlier work [8], assuming that the center oscillators (±1) and the adjacent oscillators (±2) respond with the same frequency, the following solution is proposed:

$$\begin{aligned} x_1(t) &= A\cos(\omega t) \\ x_2(t) &= B\cos(\omega t) \end{aligned} \tag{5}$$

In Eqs. (5), A and B are amplitudes of the oscillator responses and ω is the response frequency. After substituting Eqs. (5) into Eqs. (4), ω^2 can be eliminated. The higher harmonics are ignored in the analysis. In the parametrization that follows, the parameter R is introduced, where R^2 is a measure of the system's total energy. To let (A, B) be one half period out of phase, the representation (R, θ) is introduced and the oscillator amplitudes are expressed as

$$\begin{aligned} A &= R\cos(\theta) \\ B &= R\sin(\theta) \end{aligned} \tag{6}$$

The ratio of the amplitudes A and B is

$$p = \frac{B}{A} = \tan(\theta) \tag{7}$$

After substituting Eqs. (5) into Eqs. (4) and ignoring the higher harmonics, Eqs. (6) and (7) are substituted into this equation. Then, the resulting polynomial in p can be written as

$$p^4 + \gamma_3 p^3 + \gamma_2 p^2 + \gamma_1 p + \gamma_0 = 0 \tag{8}$$

wherein the different coefficients in Eq. (8) are read as

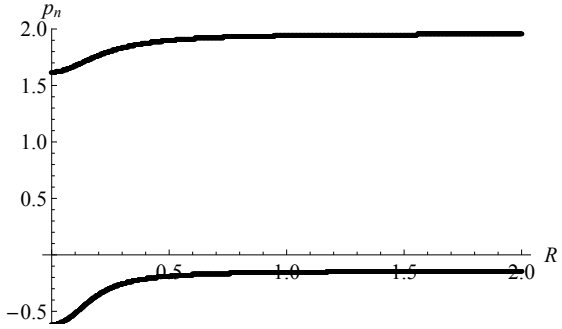

Figure 1: Roots of Eq. (8) from the restricted mode approach, for a uniform array of oscillators. The parameters used are: $\alpha_1 = 1.0$, $\alpha_2 = 0.1$, $\beta_1 = 1.0$, and $\beta_2 = 1.0$. Note that there are only two completely real roots for any particular value of R.

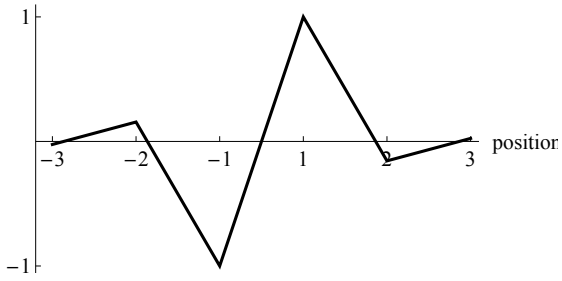

Figure 2: Profile of the P-mode ILM, as predicted from the restricted mode approach, with the parameters provided with Fig. 1. Note the zero crossing between the ±1 oscillators.

$$\begin{cases} \gamma_3 = \frac{\alpha_2 - R^2\beta_1 + R^2\beta_2}{-\alpha_2 - R^2\beta_2} \\ \gamma_2 = 0 \\ \gamma_1 = \frac{\alpha_2 + R^2\beta_1 + 6R^2\beta_2}{-\alpha_2 - R^2\beta_2} \\ \gamma_0 = \frac{\alpha_2 + R^2\beta_2}{-\alpha_2 - R^2\beta_2} \end{cases} \tag{9}$$

For the numerical studies in the next section, the following parameter values are used: $\alpha_1 = 1.0$, $\alpha_2 = 0.1$, $\beta_1 = 1.0$, and $\beta_2 = 1.0$. These values are similar to the parameters used in previous work [8], although the nonlinear coupling term is much larger here. In Fig. 1, the real roots of Eq. 8 are plotted with respect to R. It should be noted that only two of the four roots are real, while the other two form a complex conjugate pair.

To construct the profile for a P-mode ILM with an amplitude of 1, the pair (R, θ) is found, such that $A = 1$. This is performed by numerically solving

$$1 = A = R\cos(\arctan(p)) \tag{10}$$

where p is a root of Eq. (8), which is a function of R. The root is chosen to produce an ILM profile with the lowest energy level. The numerical solution to Eq. (10) leads to $R = 1.011$. On substituting these values into Eqs. (6), the

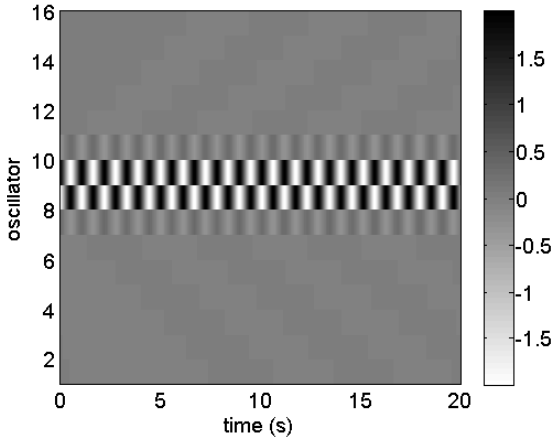

Figure 3: Time histories of oscillator responses in the unforced and undamped array. The initial state is a P-mode ILM profile, with a maximum amplitude equal to 2. The different shades of gray correspond to the oscillator displacement level.

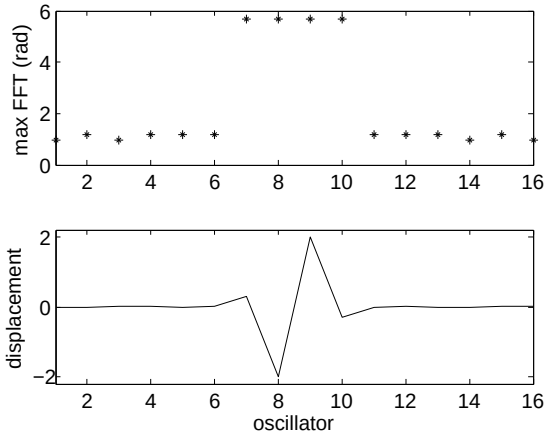

Figure 4: Oscillation frequencies and P-mode ILM profile are presented for the unforced and undamped array. In the bottom portion, the ILM profile obtained towards the end of the time history is presented. In the top portion, the oscillation frequency of each oscillator is plotted. The oscillation frequency of the main oscillators involved in the ILM oscillate with a frequency of approximately $\omega = 5.6846$ rad, while the oscillators that are not participating in the ILM oscillate at a frequency close to their linear natural frequency.

result is $A = 1.0$ and $B = -0.1560$. To find the amplitudes of the ± 3 oscillators, the obtained value of B is used to solve

$$-0.1560 = A = R\cos(\arctan(p)) \qquad (11)$$

The numerical solution to Eq. (11) gives $R = -0.1579$. Making use of these values in Eqs. (6), the authors obtain $A = -0.1560$ and $B = 0.0243$.

3. Effect of Cubic Nonlinearity on Response

In this section, a P-mode ILM profile, which has been calculated by using the restricted normal mode approach of the previous section, is used as the initial state for a numerical simulation. A large amplitude response is used, in order to highlight the effects of cubic nonlinearity on the response of the oscillator array.

In Fig. 3, the response time histories of the unforced and undamped array are presented. A gray scale color map is used to represent the different amplitude levels. In the bottom portion of Fig. 4, the ILM profile obtained towards the end of the time response is presented. In the top portion of Fig. 4, the maximum frequency component of each oscillator (as calculated from a Fast Fourier Transform) is plotted. The principal oscillators that participate in the ILM oscillate with a relatively high frequency, compared to that of the oscillators not participating in the ILM, which oscillate at a frequency near their linear natural frequency.

In order to synchronize the oscillators to the same frequency, the array was forced at the oscillation frequency of the oscillators that were participating in the unforced P-mode ILM ($\Omega = 5.6846$ rad). In Fig. 5, the time history of this forced and damped array is presented. For this numerical simulation, the values chosen are $F = 2$, $\Omega = 5.6846$ rad, and $c_i = 0.002$. A shooting method was implemented to find the response profile. The effects of forcing may be seen more clearly in Fig. 6. In the bottom portion of Fig. 6, the spatial profile obtained towards the end of the time response is presented. The effect of forcing causes a slight asymmetry in the ILM profile previously obtained. In the top portion of Fig. 6, the oscillation frequency component of each oscillator (as calculated from a Fast Fourier Transform) is plotted. As expected, the oscillation frequencies of all oscillators are entrained to the forcing frequency.

4. Concluding Remarks

A restricted normal mode analysis was implemented to study the formation of a P-mode intrinsic localized mode in a coupled, oscillator array. Since this formation is an anti-symmetric ILM, the initial assumptions differed from those used to determine the formation of the ST-mode ILM. The determined P-mode ILM profile was studied in both the unforced and forced dynamics of a cubic coupled oscillator array. When studying the formation of an ST-mode ILM with relatively low level to no cubic coupling, much of the dynamics of the ILM could be predicted by the nonlinear response of a single Duffing oscillator. For instance, the forced ST-mode is often found by forcing the oscillator array at a frequency in the region of the single Duffing oscillator's hysteresis curve where two stable solutions occur. However, it is found that the P-mode ILM has a response at a much higher frequency than the ST-mode counterpart.

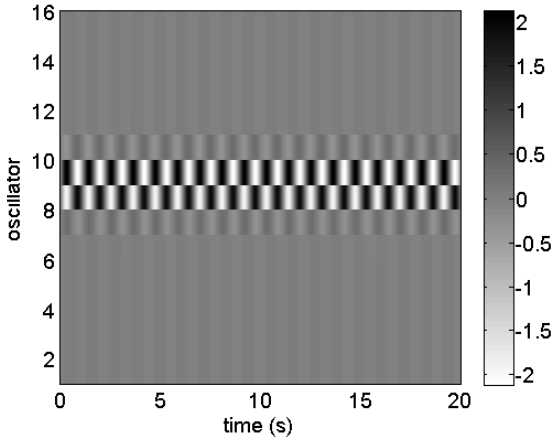

Figure 5: Time histories of oscillator responses of the forced array. For this numerical simulation, $F = 2$, $\Omega = 5.6846$ rad, and $c_i = 0.002$. The initial state is a P-mode ILM profile, with a maximum amplitude equal to 2. The results shown in thiis figure may be compared with those shown in Fig. 3.

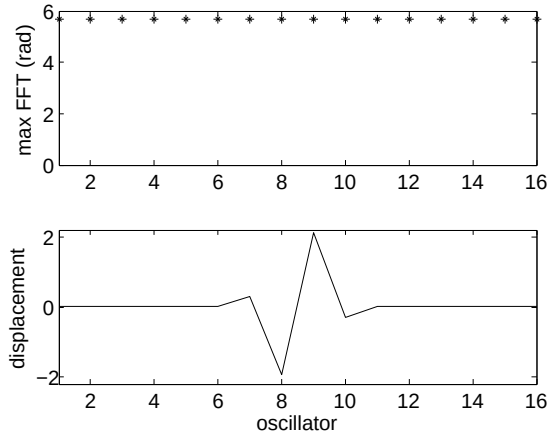

Figure 6: Oscillator response frequencies and spatial response profile are presented for the forced array. In the bottom portion, the spatial profile obtained towards the end of the time history is presented. The effect of forcing causes a slight asymmetry in the ILM profile obtained for the unforced case. In the top portion, the different oscillator response frequencies are plotted. The results shown in thiis figure may be compared with those shown in Fig. 4.

Forcing this system at the higher frequency maintains a near P-mode ILM profile. Further studies are needed to fully understand this localization phenomenon.

Acknowledgments

Partial support received for this work through NSF Grant Nos. 1414764 and CMMI 1436141, the Ford Foundation, and the Sloan Foundation is gratefully acknowledged.

References

[1] A. Yao and T. Hikihara, "Reading and writing operations of memory device in micro-electromechanical resonator," *IEICE Electronics Express*, vol. 9, no. 14, pp. 1230–1236, 2012.

[2] M. Kimura and T. Hikihara, "Experimental manipulation of intrinsic localized modes in macro-mechanical system," *Nonlinear Theory and Its Applications, IEICE*, vol. 3, no. 2, pp. 233–245, 2012.

[3] M. Sato, B. E. Hubbard, L. Q. English, A. J. Sievers, B. Ilic, D. A. Czaplewski, and H. G. Craighead, "Study of intrinsic localized vibration modes in micromechanical oscillator arrays," *Chaos*, vol. 13, pp. 702–715, 2003.

[4] M. Sato, B. E. Hubbard, and A. J. Sievers, "Colloquium: Nonlinear energy localization and its manipulation in micromechanical oscillator arrays," *Reviews of Modern Physics*, vol. 78, no. 1, pp. 137–157, 2006.

[5] J. W. Fleischer, M. Segev, N. K. Efremidis, and D. N. Christodoulides, "Observation of two-dimensional discrete solitons in optically induced nonlinear photonic lattices," *Nature*, vol. 422, pp. 147–150, 2003.

[6] A. V. Ustinov, "Imaging of discrete breathers," *Chaos*, vol. 13, no. 2, pp. 716–724, 2003.

[7] A. Dick, B. Balachandran, and C. Mote Jr, "Intrinsic localized modes in microresonator arrays and their relationship to nonlinear vibration modes," *Nonlinear Dynamics*, vol. 54, no. 1-2, pp. 13–29, 2008.

[8] B. Balachandran, E. Perkins, and T. Fitzgerald, "Response localization in micro-scale oscillator arrays: influence of cubic coupling nonlinearities," *International Journal of Dynamics and Control*, pp. 1–6, 2014.

[9] E. Perkins, M. Kimura, T. Hikihara, and B. Balachandran, "Effects of noise on intrinsic localized modes," *In preparation*, —-.

[10] M. Kimura and T. Hikihara, "Coupled cantilever array with tunable on-site nonlinearity and observation of localized oscillations," *Physics Letters A*, vol. 373, no. 14, pp. 1257–1260, 2009.